

Sensing of Large Strain Using Multiwall Carbon Nanotube/Segmented Polyurethane Composites

J.R. Bautista-Quijano, F. Avilés, J.V. Cauich-Rodriguez

Centro de Investigación Científica de Yucatán A.C., Unidad de Materiales, Calle 43 No.130, Col. Chuburna de Hidalgo. C.P. 97200, Mérida, Yucatán, México

Correspondence to: F. Avilés (E-mail: faviles@cicy.mx)

ABSTRACT: Multiwall carbon nanotube (MWCNT)/elastomeric composite films were fabricated using two segmented polyurethanes: an in-house synthesized one (SPU) and a commercial medical grade one (Tecoflex[®], TF). Electrical, mechanical, and electromechanical (piezoresistive) properties of both composites were evaluated as a function of the MWCNT weight concentration (1–10 wt %). An increase in electrical conductivity for both types of polymers was observed for MWCNT concentrations as low as 1 wt %. The electrical conductivity of MWCNT/TF composites was higher than that achieved for MWCNT/SPU composites. Mechanical properties of 8 wt % MWCNT/SPU composites showed a threefold increase in stiffness compared to neat SPU. The changes in electrical resistance of the composites showed higher sensitivity to strain for lower MWCNT concentrations. The piezoresistive signal of the composites allows to measure strains up to ~400% before electrical depercolation occurs. The strain at which electrical depercolation occurs depends on the conductivity of the composite in its unloaded state. This kind of composites may find sensing applications in prosthetics, biomedical devices, and smart textiles. © 2013 Wiley Periodicals, Inc. *J. Appl. Polym. Sci.* 130: 375–382, 2013

KEYWORDS: composites; elastomers; properties and characterization; applications; nanotubes; graphene and fullerenes

Received 6 December 2012; accepted 15 February 2013; published online 16 March 2013

DOI: 10.1002/app.39177

INTRODUCTION

Thermoplastic elastomers are known for combining their elastomeric mechanical behavior with the processability of thermoplastics. Segmented polyurethanes (SPU) are thermoplastic elastomers characterized by the urethane group, consisting of multiple alternating blocks of flexible and rigid segments.¹ In addition, SPUs have the advantage that their properties can be tailored by modifying the molar ratio of the flexible (polyol) and hard (diisocyanate) segments, which makes them suitable for a vast variety of applications. In spite of the numerous advantages of this family of polymers, they suffer from low electrical conductivity. On the other hand, it has been proved that carbon nanotubes (CNTs) can provide electrical conductivity to electrically insulating polymers,^{2,3} and they may also provide mechanically reinforcement. Coupling between the electrical conductivity and an external excitation can provide sensing capabilities to CNT composites, which can be used for measuring changes in glucose concentration,⁴ impact damage⁵ the presence of gases,⁶ or liquids.⁷ CNT/polymer composites with strain sensing capabilities have recently been also aggressively studied. For example, Wichmann et al.⁸ studied the piezoresistive properties of multiwall carbon nanotube (MWCNT)/epoxy

composites finding that a MWCNT concentration of at least 0.1 wt % is needed to obtain strain sensing capabilities; for this epoxy composite, the average gage factor ranged between 3.4–4.3 and the maximum strain measurement capability was 6%. Pham et al.⁹ reported a much lower range of strain measurement (~0.6%) but higher gage factors (1.44–15.3) using MWCNT/poly(methyl methacrylate) composites at 6–10 wt %. Zang et al.¹⁰ compared the sensitivity of MWCNT/polycarbonate composite with a commercial strain gage, finding that these nanocomposites are ~3.5 times more sensitive than a metallic strain gage. Other works where the piezoresistive properties of CNT/thermoplastics composites were studied report gage factors in the order of 0.5–1 and a maximum of 5% strain measurement capability.^{11,12} The piezoresistivity of CNT/elastomeric composites has been significantly less studied than for the case of thermoplastic or thermosetting polymers. Kang et al.¹³ found that it is possible to measure tensile and compressive strains by using a 20 wt % MWCNT/ethylene–propylene–diene rubber composite. Bokobza¹⁴ reports that cycling strain can be measured by using a 10 wt % MWCNT/styrene butadiene rubber composite. Slobodian et al.¹⁵ examined the use of a composite made from a thin buckypaper embedded in a polyurethane

matrix as a strain monitor, finding that the composite is able to monitor bending of a prosthetic knee. MWCNT/polyurethane composites have very promising piezoresistive and large strain sensing capabilities, although irreversible phenomena and hysteresis at large strains is difficult to avoid for cyclic loadings.^{15–17} Based on the existent literature, it also seems that larger concentrations of MWCNTs are required to obtain reliable piezoresistive properties using elastomers, in comparison to common thermosetting or thermoplastic polymers. However, the concentration needed using other more conventional fillers like carbon black (CB) in an elastomeric matrix is higher than that needed for MWCNTs. For example, Flandin et al.¹⁸ studied the piezoresistive properties of a CB/ethylene–octene elastomer, finding a nonlinear piezoresistive behavior and a ~300% strain measurement capability using 20 wt % of CB. On the other hand, it has been reported that it is possible to measure strains of the order of ~80% using MWCNT/thermoplastic polyurethane composites by adding only 1 wt % of MWCNTs.¹⁹

Thus, the aim of this study is to investigate the mechanical, electrical, and piezoresistive properties of two SPUs (an in-house synthesized one and a commercial one) modified by MWCNTs, and the influence of their mechanical and electrical properties on their coupled piezoresistive response.

MATERIALS

Materials Used for Composite Preparation

Commercial MWCNTs grown by chemical vapor deposition were supplied by Bayer Material Science (“Baytubes, C150P”; Bayer Material Science, Leverkusen, Germany; www.baytubes.com). The MWCNTs have inner and outer diameters of approximately 4 and 13 nm, respectively, and length in the range of 1–4 μm . The MWCNTs were subjected to a mild oxidative treatment based on nitric acid and peroxide, as reported elsewhere.²⁰ Two thermoplastic elastomers were used as matrices: (a) a commercial segmented polyurethane, Tecoflex (TF) SG-80A, with an average molecular weight (M_n) of ~40,000 g/mol supplied by “Lubrizol” (The Lubrizol Corporation, Ohio, www.lubrizol.com), and (b) an in-house synthesized segmented polyurethane (hereafter named simply “SPU”) with M_n of ~38,000 g/mol. SPU was synthesized according to Ref.²¹ using a molar ratio of 2.05:1:1 of 4,4'-methylene bis (cyclohexyl isocyanate):1,4 butanediol:poly (tethramethylene glycol ether). The first two were purchased from Sigma-Aldrich (Sigma-Aldrich, Milwaukee; www.sigmaaldrich.com) while the last one was acquired from Lyondell (Lyondell Chemical Company, Barcelona, Spain; www.lyondellbasell.com), with an approximate M_n of ~2000 g/mol. Both polymers have similar chemical composition and were chosen because of their capability to deform about 10 times their initial length.

Preparation of MWCNT Filled Polymer Composites

Composites of 1–10 wt % were prepared by dissolving 1 g of polymer (TF or SPU) in 10 mL of chloroform (CHCl_3). In parallel, MWCNTs (1–10 wt %) were dispersed in 15 mL of CHCl_3 by using an ultrasonic probe (VC750, Sonics & Materials, 150 W, 20 kHz) for 1 min and then sonicated in an ultrasonic bath (70W, 42 kHz) for 2 h. Both MWCNT/ CHCl_3 and SPU/ CHCl_3

solutions were then mixed to form a CHCl_3 /SPU/MWCNT blend which was further stirred for 2 h. In this way, 0.3 mm thick MWCNT/polymer composite films of 1–10 wt % were finally obtained by solution casting onto a Teflon mold and dried for 24 h at room temperature.

EXPERIMENTAL

Infrared Spectroscopy

Fourier transform infrared (FTIR) spectra were obtained from thin films of 5 wt % MWCNT/polymer composite deposited onto KBr pellets in the 4000–600 cm^{-1} spectral range averaging 100 scans and with resolution of 4 cm^{-1} .

Electrical Conductivity

Electrical resistance (R) of the composite films (25 mm long, 6 mm wide, and 0.3 mm thick) was measured at room temperature employing a Keithley electrometer model 6517B. Two 5 mm long silver painted areas located at the film edges were used as electrodes, leaving an effective span (L) of 15 mm. The electrical conductivity (σ_e) was calculated from the measured R as the ratio of L over the product $A \times R$, where A is the cross-sectional area of the specimen. Six replicates were measured for each composite.

Mechanical and Piezoresistive Characterization

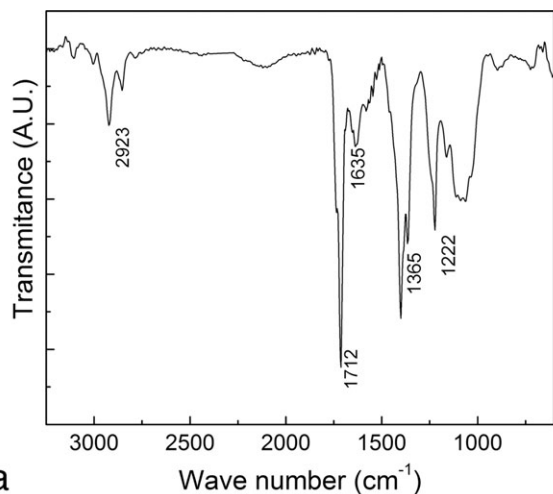
Mechanical properties were measured using a crosshead speed of 50 mm/min. Rectangular films of 60 mm length and 10 mm width were employed with 10 mm tabs at the film edges defined by adhesive tape. Since the stress (σ)–strain (ε) behavior was nonlinear, the secant modulus was obtained at strains of 100% (E_{100}) and 600% (E_{600}). Since most of the samples failed at very large strains (above 600%), the stress at $\varepsilon = 600\%$ (σ_{600}) is reported.

Tensile piezoresistive properties were evaluated using samples and test conditions similar to that used for mechanical testing. For the piezoresistive specimens, two copper wires separated 30 mm and centered at the midspan of the specimen were used as electrodes. The wires were gently pierced through the film thickness and cemented with silver paint. Electrical resistance was measured *in situ* during the tension test using a portable Fluke 289 electrometer with data logging capabilities. Six specimens were tested for each polymer and MWCNT concentration for mechanical testing and the same amount of replicates was used for piezoresistive characterization.

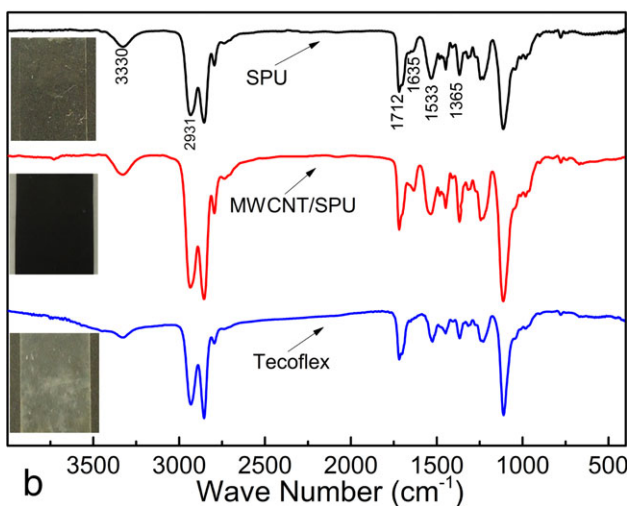
RESULTS AND DISCUSSION

Infrared Spectroscopy of Polymers and Composites

Figure 1 shows the FTIR spectra of oxidized MWCNTs [Figure 1(a)], synthesized SPU, commercial TF and a 5 wt % MWCNT/SPU composite [Figure 1(b)]. Both polymers are transparent in film geometry and become dark upon inclusion of the MWCNTs. Oxidized MWCNTs show bands corresponding to CH_2 asymmetric stretching at ~2923 cm^{-1} ,²² O–H bending at ~1365 cm^{-1} , C–O stretching at ~1222 cm^{-1} ,²³ and C=O absorptions at ~1712 cm^{-1} .^{24,25} In Figure 1(b), synthesized SPU and TF exhibit typical N–H stretching urethane absorption at ~3330 cm^{-1} ,^{26,27} and combined vibrations of bending of the N–H bond and stretching of the C–N bond at



a



b

Figure 1. FTIR spectra of MWCNTs, polymers and composites. (a) Oxidized MWCNTs, (b) SPU, TF, and 5 wt % MWCNT/SPU composite. [Color figure can be viewed in the online issue, which is available at wileyonlinelibrary.com.]

$\sim 1533\text{ cm}^{-1}$.²³ The urea group is seen at $\sim 1635\text{ cm}^{-1}$,²⁴ and the absorption at $\sim 2931\text{ cm}^{-1}$ is assigned to CH_2 from the poly(methyl-ether-glycol) used for the SPU synthesis.²²

The FTIR spectrum of the commercial TF and the in-house synthesized SPU are very similar, which confirms their similar chemical composition. The FTIR spectra of the MWCNT/SPU and MWCNT/TF (not shown) composites are similar to that of the matrix, given the low concentration of MWCNTs used and the strong IR signal of the polymer.

Electrical Conductivity

Figure 2 shows the measured DC electrical conductivity (σ_e) of MWCNT/TF and MWCNT/SPU composites at MWCNT concentrations between 0 (neat polymer) and 10 wt %. It is seen that the conductivity of TF is higher than that of SPU and that, in general, MWCNT/TF composites have higher conductivity than MWCNT/SPU composites. The difference between the conductivities of TF and SPU composites is possibly due to the presence of processing aids and/or antioxidants added to the

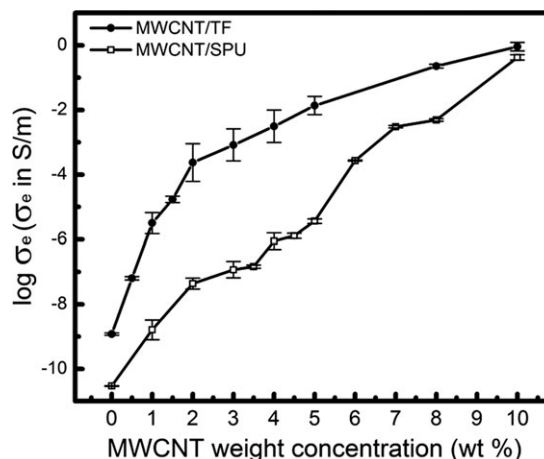


Figure 2. Electrical conductivity of SPU and TF composites as a function of MWCNT concentration.

commercial TF by the manufacturer.²⁸ These additives modify the polymer rheology upon dissolution, which in turn affects the final configuration of the MWCNT network inside the polymer.^{29,30} For both composites, at 1 wt % there is an increase in σ_e of almost two orders of magnitude, which can be associated to the formation of conductive percolating paths. However, a small number of conductive paths are formed at such a low MWCNT concentration, since the increase in electrical conductivity with respect to the neat polymer is not very pronounced at 1 wt %.

Significantly higher conductivity is observed for MWCNT composites with concentrations higher than 2 wt %. MWCNT/SPU composites with 3 wt % show a conductivity of $\sim 10^{-7}$ S/m, while the conductivity of the corresponding MWCNT/TF composites is $\sim 10^{-3}$ S/m. The maximum conductivity achieved (at 10 wt %) was 0.91 S/m for MWCNT/TF composites and 0.42 S/m for MWCNT/SPU composites. It is worth to mention that elastomeric matrices filled with carbon black^{18,31} typically require large filler concentrations (10–20 wt %) to achieve similar levels of conductivity than those found in this study.

Mechanical Properties

The mechanical behavior of the investigated composites is depicted in Figure 3. Figure 3(a) shows representative stress (σ)–strain (ϵ) curves of 0, 4, 5, and 8 wt % MWCNT/TF composites, while Figure 3(b) shows the corresponding curves for MWCNT/SPU composites.

MWCNT/TF composites with 4 wt %, Figure 3(a), show reduced tensile mechanical properties with respect to the neat polymer; however, at and above 5 wt %, MWCNT/TF composites show a reinforcement effect especially for properties at 600% strain (E_{600} , σ_{600}). This suggests that there is a minimum MWCNT weight concentration needed to effectively reinforce the polyurethane matrix. Increasing the amount of MWCNTs into a thermoplastic polyurethane leads to a state in which the MWCNTs form a continuous percolated network. Above this concentration an increase in the mechanical properties of the composite is expected due to the formation of two co-continuous phases.³² It has also been reported that the presence of

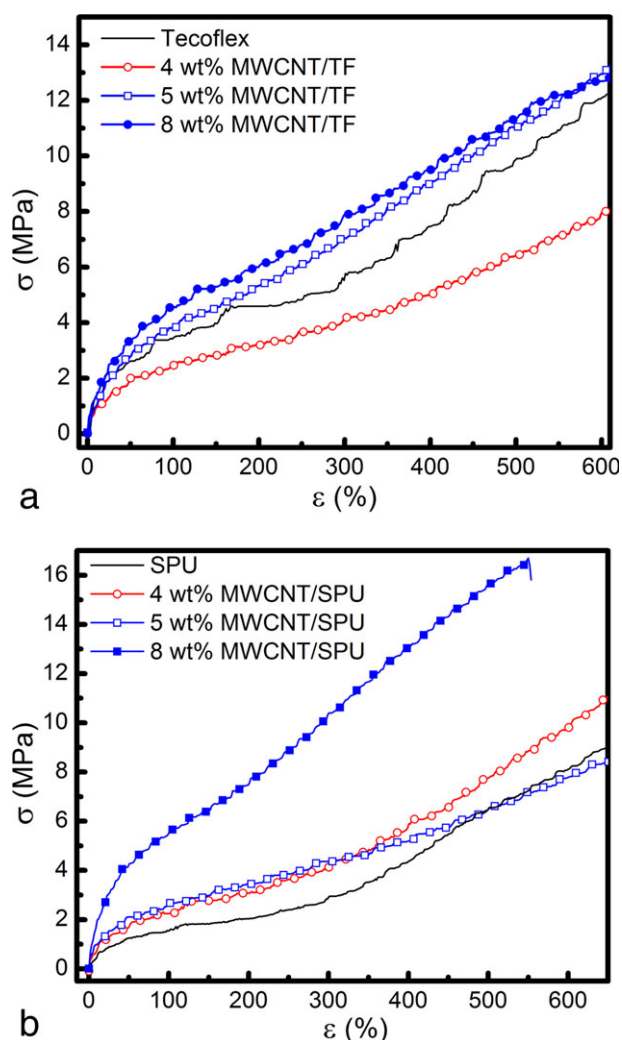


Figure 3. Representative tensile stress–strain curves of MWCNTs composites. (a) MWCNT/TF and (b) MWCNT/SPU. [Color figure can be viewed in the online issue, which is available at wileyonlinelibrary.com.]

MWCNTs may enhance the crystallinity of soft segments in segmented polyurethanes during elongation of the composites.³³ Both phenomena may lead to a stiffening effect in the MWCNT/polymer composites investigated here, and both of them require a concentration of MWCNTs above electrical percolation. MWCNT/TF composites loaded with 5 and 8 wt % show similar mechanical properties, although MWCNT/TF composites at 8 wt % show slightly larger stiffening effects. For 8 wt % MWCNT/TF composites, E_{100} was 1.3 times higher than the corresponding value for neat TF, whereas E_{600} and σ_{600} increased 10%. For MWCNT/SPU composites [Figure 3(b)] a reinforcing effect (stiffening) is observed for concentrations as low as 4 wt %. 4 and 5 wt % MWCNT/SPU composites show a value of E_{100} which is ~ 1.6 times larger than the E_{100} of neat SPU. The largest stiffening effect of all examined materials occurred for SPU composites with 8 wt %, which show a threefold increase in E_{100} , and a twofold increase in E_{600} and σ_{600} with respect to the neat SPU. In the case of 8 wt % MWCNT/SPU composites, E_{600} , and σ_{600} were actually taken at $\epsilon = 550\%$

since the specimens failed at this strain. Thus, the large stiffening effect caused by the MWCNTs in the SPU matrix comes with the concomitant effect of reduced ultimate strain. The content of flexible (soft) and rigid (hard) segments influence the mechanical properties of segmented polyurethanes and there is an intrinsic incompatibility between the hard and soft segments, which tends to form a two-phase microstructure.³⁴ It has been reported that MWCNTs tend to present stronger interactions with the hard segments in a SPU³⁵ and also that the crystallinity of the soft segments may increase because of the nucleation effect of the CNTs.³³ Therefore, the stiffening effect of the MWCNTs for segmented polyurethanes may be explained mainly by the interaction between the carboxylic groups on the surface of the functionalized MWCNTs with the hard segments of the segmented polyurethane, although other indirect phenomena such as the increase in soft segment crystallinity and strain-induced crystallization may also be relevant.^{32–36}

Piezoresistive Properties

The coupled electromechanical properties of composites with conductivity $\geq 10^{-4}$ S/m were characterized by tensile piezoresistive testing. This corresponds to TF composites with MWCNT concentration ≥ 3 wt % and SPU composites with MWCNT concentration ≥ 6 wt %. Figure 4 shows typical

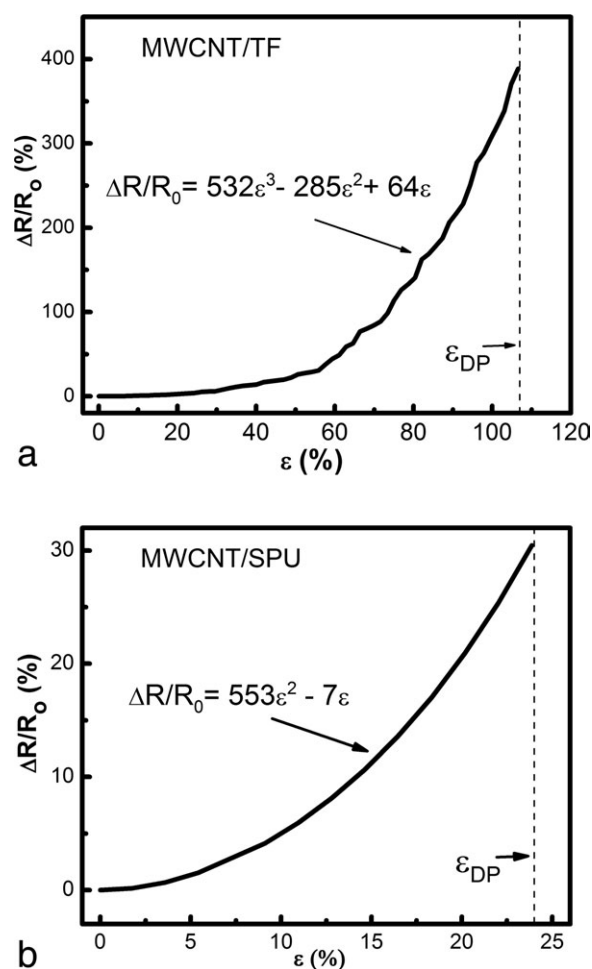


Figure 4. Representative piezoresistive curves of 6 wt % MWCNT composites. (a) MWCNT/TF and (b) MWCNT/SPU.

piezoresistive curves ($\Delta R/R_0$ vs. ε , where R_0 is the electrical resistance in the unloaded state) for 6 wt % composites with TF [Figure 4(a)] and SPU [Figure 4(b)] matrices. $\Delta R/R_0$ increases with increased ε , suggesting that the distance between the nanotubes is also increased leading to a higher electrical resistance. Once the applied strain reaches a critical value, the separation between MWCNTs is so large that the electrically percolating network breaks down. This behavior occurs in highly deformable polymers and has been named “electrical depercolation.”¹⁸ The strain at which electrical depercolation occurs is identified here by the label “ ε_{DP} ” as indicated in Figure 4. In this study, ε_{DP} was defined as the strain at which the conductivity of the composites decreases below 10^{-5} S/m, which is close to the conductivity threshold reported for the transition from semiconductors to electrically insulating materials.³⁷ For the geometry of the samples examined, this value corresponds to an electrical resistance of the order of $\sim 10^2$ M Ω which is also a practical limit for laboratory measurements. The complete piezoresistive curves showed in Figure 4 can be fitted to a cubic (MWCNT/TF) or quadratic (MWCNT/SPU) polynomial functions.

In Figure 4, the investigated composites have a large strain capability with a non-linear piezoresistive behavior. Because of the large axial strain achieved by elastomers and their high Poisson’s ratio,^{34,38} a large reduction in cross-sectional area is also expected. However, as pointed out in Ref. ³⁹, the strain transferred to the CNT is very low and this geometric contribution is minor in the measured piezoresistive response. Factors such as variations in CNT-to-CNT distance, tunneling and CNT-to-CNT contact resistance, are accepted among the major contributing factors to the piezoresistivity of polymer composites.^{39–42} According to Zhang et al.⁴², for MWCNT/polyurethane composites, the changes in electrical resistance during stretching can be described by the deformation of the MWCNT network and the increase in the tunnel junction gap. At large strains, the second behavior may be dominant.⁴² In our case, the reduction in cross-sectional area may tend to align the MWCNTs in the load direction³³ and such rotations may also influence ΔR .⁴¹

Table I list $\Delta R/R_0$ as function of ε for the composites showed in Figure 4. As seen from this table, 6 wt % MWCNT/SPU composites are more sensitive than 6 wt % MWCNT/TF ones, since for any fixed strain $\Delta R/R_0$ is higher for SPU composites.

This behavior can be due to the combination of the lower electrical conductivity (Figure 2) and lower stiffness (Figure 3) of MWCNT/SPU composites. At 10% strain $\Delta R/R_0$ of MWCNT/SPU is 4.76% ($\Delta R/\varepsilon R_0 = 0.48$) whereas for MWCNT/TF $\Delta R/R_0$ is only 0.91% ($\Delta R/\varepsilon R_0 = 0.091$). The strain sensitivity, quantified by the factor $\Delta R/\varepsilon R_0$ in Table I, increases with increased applied strain. However, although the strain sensitivity is significantly higher for MWCNT/SPU composites, the depercolation strain (ε_{DP}) is higher for MWCNT/TF composites. This is likely due to the higher conductivity of the TF composites. For the case of 6 wt % MWCNT/TF composites, ε_{DP} is $\sim 105\%$ while for MWCNT/SPU composites at the same MWCNT concentration ε_{DP} is $\sim 25\%$ (Figure 4).

Figure 5 shows the piezoresistive [Figure 5(a)] and corresponding stress–strain [Figure 5(b)] curves of MWCNT/TF composites at several MWCNT concentrations. All piezoresistive curves can be fitted to polynomial functions of order 2 to 4.

From Figure 5, it is concluded that the 3 wt % MWCNT/TF composite is the most sensitive one among the TF composites, since exhibits higher $\Delta R/R_0$ than the other composites for a fixed ε . This higher sensitivity correlates with its lower electrical conductivity (Figure 2). For $\varepsilon = 35\%$, $\Delta R/\varepsilon R_0$ for this composite is ~ 0.30 . On the other hand, this composite also exhibits the lowest ε_{DP} ($\sim 40\%$) of the TF composites examined, which seems to correlate also with its lowest electrical conductivity. For MWCNT concentrations above 8 wt %, the measured ΔR signal fluctuates as shown in Figure 5(a), indicating that the CNT network is densely packed. Such a high MWCNT concentrations may not be adequate for sensing applications of these MWCNT composites.

The piezoresistive [Figure 6(a)] and corresponding stress–strain [Figure 6(b)] curves of MWCNT/SPU composites at different MWCNT concentrations are shown in Figure 6. The piezoresistive curves of the MWCNT/SPU can be fitted to polynomial functions of order 2 to 4.

According to Figure 6(a), the most sensitive MWCNT/SPU composite is again the one with the lowest concentration of MWCNT (6 wt %). ε_{DP} also increases by increasing the MWCNT concentration, which in turns increases the conductivity of the composite. This behavior is in agreement with the piezoresistive properties obtained for MWCNT/TF composites, suggesting that the sensitivity is reduced and the depercolation

Table I. $\Delta R/R_0$ as Function of ε for 6 wt % MWCNT/TF and MWCNT/SPU Composites

ε (%)	$\Delta R/R_0$ (%)		$\Delta R/\varepsilon R_0$	
	MWCNT/TF	MWCNT/SPU	MWCNT/TF	MWCNT/SPU
10	0.91 ± 0.25	4.76 ± 1.05	0.091 ± .025	0.48 ± 0.105
15	1.94 ± 0.52	10.9 ± 0.87	0.13 ± 0.035	0.73 ± 0.058
20	3.37 ± 0.77	20.2 ± 1.08	0.17 ± 0.039	1.01 ± 0.054
25	5.10 ± 1.13	31.5 ± 2.63	0.20 ± 0.045	1.26 ± 0.105
30	7.21 ± 0.94	-	0.24 ± 0.031	-
90	237.2 ± 76.4	-	2.64 ± 0.85	-

- = ε above ε_{DP} .

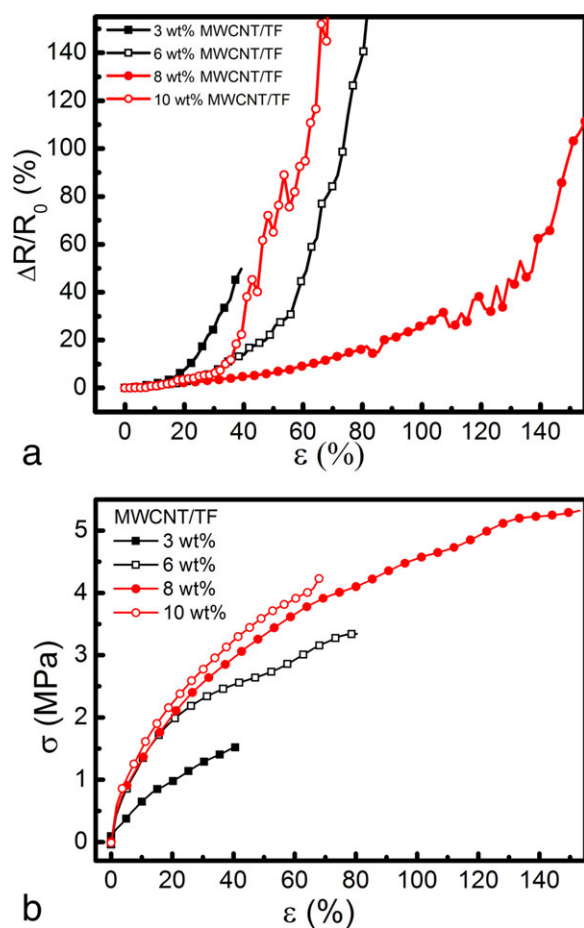


Figure 5. Electrical and mechanical responses of MWCNT/TF composites as a function of applied strain. (a) Electrical response and (b) corresponding stress–strain curve. [Color figure can be viewed in the online issue, which is available at wileyonlinelibrary.com.]

strain increased by increasing the concentration of MWCNTs. Increasing the MWCNT concentration yields stiffer composites (less CNT mobility) and a densely packed network (less change in ΔR), which may justify this experimental observation.

Further analysis of the depercolation strain is possible with the assistance of Figure 7, which shows the values of ϵ_{DP} for MWCNT/TF and MWCNT/SPU composites as a function of the MWCNT concentration. The highest ϵ_{DP} observed for MWCNT/TF composites ($\sim 400\%$) occurred at 8 wt %, while the lowest ϵ_{DP} (40%) was obtained at 3 wt %.

The largest strain measurement capability found herein ($\sim 400\%$, dictated by ϵ_{DP}) is larger than that reported for the majority of MWCNT/elastomeric composites,^{16,17,19} and is similar only to that reported for MWCNT composites with an especially designed (layered) architecture.^{15,43} For MWCNT/TF composites, ϵ_{DP} increases when the MWCNT content increases from 3 wt % to 8 wt %, but decreases after 8 wt %. This behavior may be explained by clustering and network saturation at such high MWCNT concentrations. It is possible that above 8 wt %, clusters and zones deficient of MWCNTs are formed, increasing the probability of breaking the percolated network upon strain application.

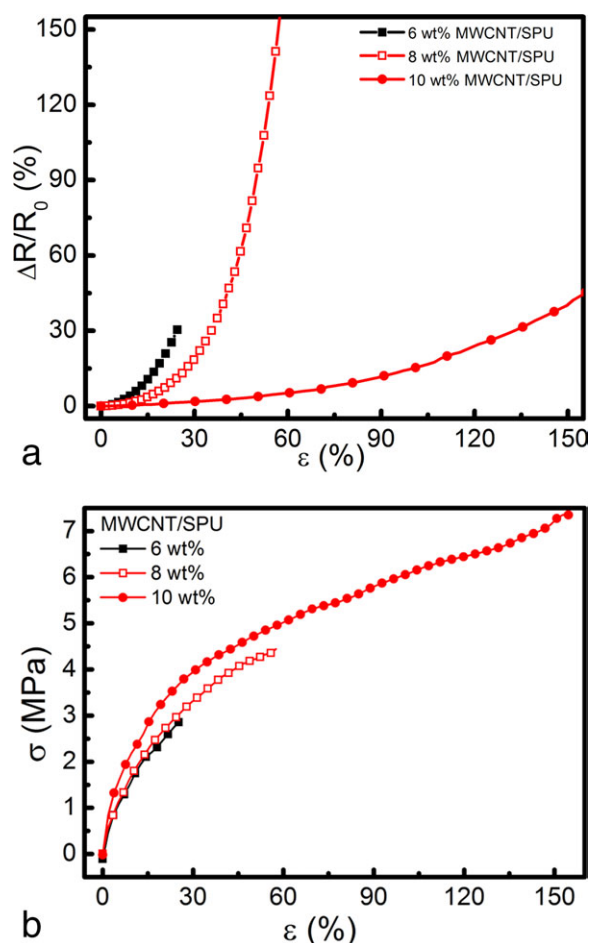


Figure 6. Electrical and mechanical responses of MWCNT/SPU composites as a function of applied strain. (a) Electrical response and (b) corresponding stress–strain curve. [Color figure can be viewed in the online issue, which is available at wileyonlinelibrary.com.]

For MWCNT/SPU composites the lowest ϵ_{DP} ($\sim 25\%$) occurred at 6 wt % while the highest ϵ_{DP} ($\sim 200\%$) was found at 10 wt %. For these composites (which are less conductive than

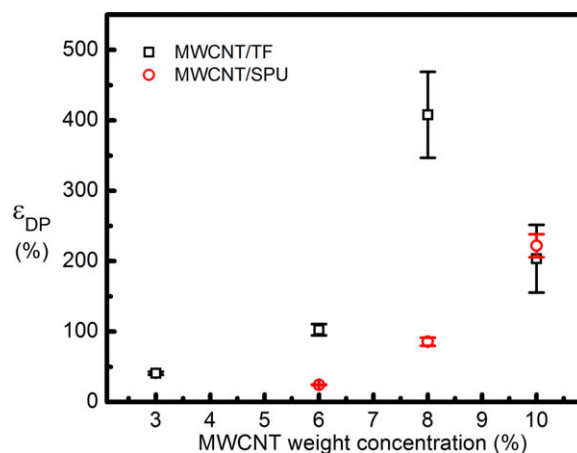


Figure 7. Depercolation strain as a function of MWCNT wt % for MWCNT/TF and MWCNT/SPU composites. [Color figure can be viewed in the online issue, which is available at wileyonlinelibrary.com.]

the TF ones), ϵ_{DP} increases monotonically as the MWCNT content increases, which is possible due to the increase in electrical conductivity of the composites with increased MWCNT concentration.

CONCLUSIONS

Segmented polyurethane/MWCNT composites were manufactured and characterized electrically, mechanically, and electro-mechanically. Two kinds of segmented polyurethanes were employed, an in-house synthesized one (SPU) and a commercial one (Tecoflex, TF). The influence of the mechanical and electrical properties on the coupled piezoresistive behavior of the composites, and the strain at electrical depercolation as a function of the MWCNT concentration and matrix type were of main interest. Electrical percolation was found around 1 wt % and the electrical conductivity of composites fabricated with TF was higher than those fabricated with the in-house synthesized SPU. The maximum conductivity achieved was 0.91 S/m for 10 wt % MWCNT/TF composites, and 0.42 S/m for 10 wt % MWCNT/SPU composites. Mechanical reinforcement was evident as a stiffening effect in both polymers at MWCNT concentrations ≥ 5 wt %; the stiffening effect was more notorious for higher MWCNT concentration (up to 8 wt %) and for SPU composites. Higher piezoresistive sensitivity was obtained for SPU composites, reaching values of $\Delta R/R_0 \sim 30\%$ for 25% strain, and changes in electrical resistance as high as $\sim 200\%$ with respect to its original value for $\sim 180\%$ strain. The piezoresistive properties obtained suggest that as the MWCNT concentration increases, the piezoresistive sensitivity of the polyurethane composites is reduced. The strain at electrical depercolation varied from $\sim 25\%$ to $\sim 400\%$, depending on the initial electrical conductivity of the composite. Composites with higher electrical conductivity in its unstrained state reached higher values of depercolation strain. The large deformation capability of these composites and the large changes in electrical resistance produced by the strain application makes them a suitable candidates as strain sensing elements in biomedical, structural health monitoring, and smart textiles applications.

ACKNOWLEDGMENTS

This study was supported by CONACYT (Mexico). Technical assistance of A. May-Pat, L.H. Chan-Chan and R.F. Vargas-Coronado is gratefully acknowledged.

REFERENCES

- Hepburn C. Polyurethane elastomers; Applied Science Publishers: London, 1982.
- Thostenson, E.T.; Li, C.; Chou, T.W. *Compos. Sci. Technol.* **2004**, *65*, 491.
- Terrones, M. *Annual. Rev. Mater. Sci.* **2003**, *33*, 419.
- Singh K.; Singh B.P.; Chauhan R.; Basu, T. *J. App. Polym. Sci.* **2012**, *125*, E235.
- Arronche L.; La Saponara V.; Yesil S.; Bayram G. *J. App. Polym. Sci.* **2012**, DOI: 10.1002/app.38448.
- Olejnik, R.; Slobodian, P.; Riha, P.; Machovsky, M. *J. App. Polym. Sci.* **2012**, *126*, 21.
- Pötschke, P.; Kobashi, K.; Villmow, T.; Andres, T.; Pavia, M.C.; Covas, J.A. *Compos. Sci. Technol.* **2011**, *71*, 1451.
- Wichmann, M.H.G.; Buschhorn, S.T.; Gehrman, J.; Schulte, K. *Phys. Rev. B* **2009**, *84*, 245437.
- Pham, G.T.; Park, Y.B.; Liang, Z.; Zhang, C.; Wang. *Compos. Part B Eng.* **2008**, *39*, 209.
- Zang, W.; Suhr, J.; Koratkar, N. *J. Nanosci. Nanotech.* **2006**, *6*, 960.
- Bautista-Quijano, J.R.; Aviles, F.; Aguilar, J.O.; Tapia, A. *Sensors Actuat. A Phys.* **2010**, *159*, 135.
- Oliva-Avilés, A.I.; Avilés, F.; Sosa, V. *Carbon* **2011**, *49*, 2989.
- Kang, I.; Khaleque, M.A.; Yoo, Y.; Yoon, P.J.; Kim, S.Y.; Lim, K.T. *Compos. Part A Appl. Sci.* **2011**, *42*, 623.
- Bokobza, L. *Polymer* **2007**, *48*, 4907.
- Slobodian, P.; Riha, P.; Saha, P. *Carbon* **2012**, *50*, 3446.
- Bilotti, E.; Zhang, R.; Deng, H.; Baxendale, M.; Peijs, T. *J. Mater. Chem.* **2010**, *20*, 9449.
- Zhang, R.; Deng, H.; Valenca, R.; Jin, J.; Fu, Q.; Bilotti, E.; Peijs, T. *Compos. Sci. Technol.* **2013**, *74*, 1.
- Flandin, L.; Hiltner, A.; Baer, E. *Polymer* **2001**, *42*, 827.
- Zhang, R. PhD Thesis. Conductive TPU/CNT composites for strain sensing; Queen Mary, University of London UK; School of Engineering and Materials Science: London, **2009**.
- Avilés, F.; Cauich-Rodríguez, J.V.; Moo-Tah, L.; May-Pat A.; Vargas-Coronado, R. *Carbon* **2009**, *47*, 2970.
- Moo-Espinosa, J.M.; Solís-Correa, R.; Vargas-Coronado, R.; Cervantes-Uc, J.M.; Cauich-Rodríguez, J.V.; Quintana-Owen, P.; Aguilar-Santamaria, M.A.; Fernandez-Gutierrez, M.; San Roman del Barrio, J. *J. Biomater. Appl.* DOI: 10.1177/0885328212436706.
- Cervantes-Uc, J. M.; Moo-Espinosa J. I.; Cauich-Rodríguez, J. V.; Ávila-Ortega A.; Vázquez-Torres H.; Marcos-Fernández A.; San Román J. *Polym. Degrad. Stab.* **2009**, *94*, 1666.
- Irusta, L.; Fernandez-Berridi M. *J. Polym. Degrad. Stab.* **1999**, *63*, 113.
- Chan-Chan, L. H.; Solis-Correa, R.; Vargas-Coronado R. F.; Cervances-Uc, J. M.; Cauich-Rodríguez, J. V.; Quintana, P.; Bartolo-Pérez P. *Acta Biomater.* **2010**, *6*, 2035.
- Elidrissi, A.; Krim, O.; Ouslimane, S.; Berrabeh, M.; Touzani R. *J. Appl. Polym. Sci.* **2007**, *105*, 1623.
- Biamond, G. J. E.; Braspenning K.; Gaymans, R. J. *J. Appl. Polym. Sci.* **2008**, *107*, 2180.
- Solis-Correa, R. E.; Vargas-Coronado R. F.; Aguilar-Vega, M.; Cauich-Rodríguez, J. V.; San Román, J.; Marcos, A. *J. Biomater. Sci. Polym. E.* **2007**, *561*.
- Sreenivasan, K. *Chromatographia* **1991**, *32*, 285.
- Pötschke, P.; Fornes T. D.; Paul D. R. *Polymer* **2002**, *43*, 3247.
- Li, J.; Ma, P. C.; Chow, W. S.; To, C. K.; Tang, B. Z.; Kim, J.-K. *Adv. Funct. Mater.* **2007**, *17*, 3207.
- Luheng, W.; Tianhuai, D.; Peng, W. *Carbon* **2009**, *47*, 3151.

32. Fernández-d'arlas, B.; Khan, U.; Rueda, L.; Martin L.; Ramos, J. A.; Coleman J. N.; González M. L.; Valea A.; Mongragon I.; Corcuera M. A.; Eceiza A. *Compos. Sci. Technol.* **2012**, *72*, 235.
33. Koerner, H.; Liu, W.; Alexander, M.; Mirau, P.; Dowty, H.; Vaia, R. A. *Polymer* **2005**, *46*, 4405.
34. Qi, H. J.; Boyce, M. C. *Mech. Mater.* **2005**, *37*, 817.
35. Fernández-d'Arlas, B.; Khan, U.; Rueda, L.; Coleman, J. N.; Mondragon, I.; Corcuera, M. A.; Eceiza, A. *Compos. Sci. Technol.* **2011**, *71*, 1030.
36. Sahoo, N.G.; Jung, Y.C.; Yoo, H.J.; Cho, J.W. *Macromol. Chem. Phys.* **2006**, *207*, 1773.
37. Callister W. D. In *Fundamentals of Material Science and Engineering*; Anderson W., Ed.; Wiley: New York, **2001**.
38. Tsukinovsky D.; Zaretsky E.; Rutkevich I. *J. Phys. IV* **1997**, *7*, C3–335.
39. Oliva-Avilés, A. I.; Avilés, F.; Seidel, G. D.; Sosa V. *Compos. Part B Eng.* **2013**, *47*, 200.
40. Dharap, P; Li, Z; Nagarajiah, S; Barrera, E.V. *Nanotechnology* **2004**, *15*, 379.
41. Rahman, R; Servati, P. *Nanotechnology* **2012**, *23*, 055703.
42. Zhang, R.; Baxendale, M.; Peijs, T. *Phys. Rev. B* **2007**, *76*, 195433.
43. Fan Q.; Qin, Z.; Gao, S.; Yongtao W.; Pionteck, J.; Mäder, E.; Zhu, M. *Carbon* **2012**, *50*, 4085.